Mol Biotechnol (2015) 57:982–992
DOI 10.1007/s12033-015-9891-0

RESEARCH

Potato Virus M-Like Nanoparticles: Construction and Characterization

Ieva Kalnciema[1] · Ina Balke[1] · Dace Skrastina[1] · Velta Ose[1] · Andris Zeltins[1]

Published online: 7 September 2015

Abstract Virus-like particles (VLPs) are multisubunit self-assembly competent protein structures with identical or highly related overall structure to their corresponding native viruses. To construct a new filamentous VLP carrier, the coat protein (CP) gene from potato virus M (PVM) was amplified from infected potato plants, cloned, and expressed in *Escherichia coli* cells. As demonstrated by electron microscopy analysis, the PVM CP self-assembles into filamentous PVM-like particles, which are mostly 100–300 nm in length. Adding short Gly-Ser peptide at the C-terminus of the PVM, CP formed short VLPs, whereas peptide and protein A Z-domain fusions at the CP N-terminus retained its ability to form typical PVM VLPs. The PVM-derived VLP carrier accommodates up to 78 amino acid-long foreign sequences on its surface and can be produced in technologically significant amounts. PVM-like particles are stable at physiological conditions and also, apparently do not become disassembled in high salt and high pH solutions as well as in the presence of EDTA or reducing agents. Despite partial proteolytic processing of doubled Z-domain fused to PVM VLPs, the rabbit IgGs specifically bind to the particles, which demonstrates the functional activity and surface location of the Z-domain in the PVM VLP structure. Therefore, PVM VLPs may be recognized as powerful structural blocks for new human-made nanomaterials.

Keywords Plant · Virus-like · Carlavirus · Protein A

Introduction

From a technological perspective, virus-like particles (VLPs) can be regarded as multisubunit, self-assembly competent protein structures on the nanometer scale with identical or with an extremely similar overall structure with their corresponding native viruses, which represent nearly ideal building blocks to create a wide variety of new nanomaterials for different purposes [1, 2]. First, VLPs are well known as active compounds in commercial vaccines against hepatitis B and human papilloma viruses and recently, against the hepatitis E virus [3]. Several new VLP-based vaccine candidates have entered clinical studies with the goal of developing vaccines for medical and veterinary purposes (see [4, 5] for reviews, respectively).

Historically, one of the first recombinant VLPs was obtained from the coat protein (CP) complementary DNA (cDNA) copy of the tobacco mosaic virus (TMV) nearly 30 years ago [6]. Since that time, many plant VLPs have been suggested for use in nanotechnology applications as immunologically active carriers of peptides and whole proteins and as protein containers for the encapsidation of nucleic acids, proteins, metals, and other active substances depending on the intended downstream application. In

Electronic supplementary material The online version of this article (doi:10.1007/s12033-015-9891-0) contains supplementary material, which is available to authorized users.

✉ Andris Zeltins
anze@biomed.lu.lv

Ieva Kalnciema
kalnciema@biomed.lu.lv

Ina Balke
inab@biomed.lu.lv

Dace Skrastina
daceskr@biomed.lu.lv

Velta Ose
velta@biomed.lu.lv

[1] Latvian Biomedical Research and Study Centre, Ratsupites 1, Riga 1067, Latvia

addition, plant VLPs can also be incorporated into supramolecular structures, which create different nanomaterials with defined properties [7]. The majority of plant VLPs suggested for different applications are icosahedral with known three-dimensional (3D) structure models, which is one of the necessary prerequisites to create virus-based nanomaterials. However, out of the 25 VLPs obtained from the plant virus CP gene expression in heterologous cell systems, approximately, 40 % of these were obtained from filamentous or rod-shaped viruses [1]. The 3D structure models of these viruses are available only in a limited number of cases: the structures of native TMV [8], the soybean mosaic virus (SBM), and the potato virus X (PVX) [9] were suggested based on X-ray fiber diffraction and cryo-electron microscopy studies. Despite limited structural information, several filamentous viruses, which are both capable of replication and in the form of their corresponding VLP derivatives, have been developed as vaccine candidates. These viral derivatives have been shown to expose different medically relevant epitopes or protein domains on their surface as N- or C-terminal genetic fusions with the corresponding viral CPs, e.g., PVX [10], papaya mosaic virus (PapMV) [11], potato virus Y (PVY) [12], Johnson grass mosaic virus [13], TMV [14, 15], etc. The latest studies suggest that elongated, filamentous nanoparticles have advantages over isometric VLPs, such as being a more effective epitope presentation to the target cells and increased tumor homing and immune evasion ([16] and references cited herein).

The potato virus M (PVM) belongs to the genus *Carlavirus* in the family *Betaflexiviridae* [17, 18]. Morphologically, native PVM particles are rod-shaped or slightly curved filaments with dimensions of 650 × 12 nm [19]. PVM virions contain a linear, single-stranded, positive-sense RNA genome of approximately 8.5 kb, which is organized in six open reading frames (ORFs). ORF1 is coding for a polypeptide involved in RNA replication. The overlapping ORFs 2, 3, and 4 (triple gene block—TGB) encode three putative proteins of 25, 12, and 7 kDa, which are supposed to be involved in cell-to-cell movement. ORFs 5 and 6 encode the 34 kDa CP and a nucleic acid binding protein (11 kDa), respectively. Native carlavirus helical virions consist of more than 1600 CP subunits (ca. 8 subunits per turn) [20]; the virus yield obtained from infected plant tissue is less than 50 μg of virus per gram of tissue [21]. As for most filamentous viruses, the 3D structure model for the PVM is unknown.

For biotechnological applications of *Carlavirus* representatives, a gene-silencing vector based on a full-length genomic clone of the poplar mosaic virus (PopMV) was constructed [22]. With the goal to obtain purified viral CPs for subsequent immunizations and antibody productions, carlavirus CP gene expressions in bacterial hosts have been previously reported; however, CPs have been found in the form of inclusion bodies; VLPs have not been identified [23, 24].

Despite the availability of numerous VLPs that possess different advantages, only a few of them can be characterized as being nearly universal [1]. Therefore, the interest in the usage of new VLP carriers for immunological and nanotechnological applications is still growing. Here, we report the cloning of PVM CP-encoding cDNA from PVM-infected potato plantlets and present data on the properties of a new plant virus-based VLP carrier. The PVM-like particles can accommodate up to 78 AA-long foreign protein sequences on the surface of filamentous VLPs and can be produced in *E. coli* cells with comparably high yields.

Materials and Methods

Cloning of PVM CP-Encoding cDNA

Potato meristem plantlets infected with PVM were obtained from MSc. I. Mezaka (State Priekuli Plant Breeding Institute, Latvia). All chemicals were purchased from Sigma (Saint Louis, USA), and enzymes were purchased from Thermo Scientific (Fermentas, Vilnius, Lithuania) unless otherwise indicated. The total RNA from infected plant material was isolated using TRI reagent in accordance with the manufacturer's recommendations. For cDNA synthesis from total RNA, M-MuLV H (−) reverse transcriptase and random hexamer primers were used. For cloning of the PVM CP gene, the primer sequences were chosen from conserved regions surrounding the CP gene following the analysis of PVM sequences from GenBank. After PVM CP cDNA amplification using the 1F/1R primer pair (Suppl. Table 1) and Taq DNA polymerase, the corresponding PCR product was cloned into the pTZ57R/T vector (Thermo Scientific, Vilnius, Lithuania) using *E.coli* XL1-Blue cells as a host for cloning and plasmid amplification. To obtain the cDNA clone without RT-PCR errors, several CP gene-containing plasmids were sequenced using a BigDye cycle sequencing kit and an ABI Prism 3100 Genetic analyzer (Applied Biosystems, Carlsbad, USA). The cDNA sequence of PVM CP was submitted to the Genbank nucleotide sequence database and can be found under accession number GQ496609.

Construction of Plasmids for the Expression of the PVM CP Gene and Its Derivates

PCR mutagenesis and subcloning procedures for PVM CP cDNA were performed as previously described [25]. To obtain a full-length PVM CP clone with NcoI/HindIII sites

for subsequent cloning in expression vector pET28a+ (Novagen, San Diego, USA), the 2F/2R primer pair (Suppl. Table 1) was used in the PCR. After subcloning of the PCR product in the pTZ57R/T vector, the correct clone was identified by sequencing. The verified PVM CP gene was then subcloned into NcoI/HindIII sites of the pET28a+ vector, which resulted in the plasmid pET-PvmCP.

To introduce N-terminal G4S linker coding sequences into the PVM CP gene, two-step PCR mutagenesis was necessary. In the first step, the G4S linker cDNA was amplified from previously constructed pET-PvyCP-NG4S [12] and PVM CP gene 5′end using primer pairs 3F/3R and 4F/4R (Suppl. Table 1). Then, both PCR fragments were purified, fused in the PCR reaction, and amplified using primers 3F and 4R. The resulting NcoI/EcoRI-cleaved PCR product was further subcloned into the pET-PvmCP, which replaced the 5′end NcoI/EcoRI fragment. A similar strategy was chosen to introduce the C-terminal G4S coding sequence in the PVM CP gene: the 3′end of the PVM CP gene was amplified by 5F/5R primers; the G4S linker sequence was synthesized from the pET-PvyCP-CG4S template [12] (primers 6F/6R), then both fragments were joined and amplified using primers 5F and 6R; and finally, the BsrGI/HindIII fragment in the pET-PvmCP was replaced by the PCR product cut with the same restriction enzymes. The compliance of the resulting expression plasmids pET-PvmCP-NG4S and pET-PvmCP-CG4S was confirmed by BigDye cycle sequencing.

The cDNA of immunoglobulin G (IgG) binding doubled Z-domain (ZZ-domain) of protein A from *Staphylococcus aureus* flanked by NcoI and BamHI restriction sites was amplified using primer pair 7F/7R and plasmid pEZZ18 (GE Healthcare) as a template. Then, the PCR fragment was subcloned into pET-PvmCP-NG4S at the same sites at the 5′end of the gene. All DNA maps with relevant restriction enzyme sites and the AA sequences of the PVM CP-derived proteins constructed for this study can be found in Suppl. Figure 1.

Synthesis and Purification of PVM CP-Derived Proteins

For target protein production, *E. coli* BL21(DE3) cells were transformed with the corresponding plasmid DNA. *E.coli* cultures were grown in 2× TY medium (1.6 % Trypton, 1 % yeast extract, 0.5 % NaCl, 0.1 % glucose), which contained kanamycin (25 mg/l) on a rotary shaker (200 rev/min; Infors, Bottmingen, Switzerland) at 30 °C to an OD(600) of 0.8. Target protein synthesis was then induced with 0.2 mM IPTG, and the medium was supplemented with 2 mM $CaCl_2$ and 5 mM $MgCl_2$. The cultivation continued on the rotary shaker at 20 °C for 18 h. The resulting biomass was collected by low-speed centrifugation and was frozen at −20 °C. After being thawed on ice, the cells were suspended in a Tris buffer (20 mM, pH of 8.0; 6 ml for 1 g wet biomass) containing 5 mM mercaptoethanol and 1 mM PMSF and were disrupted by ultrasonic treatment using a Covaris S220 device (Woburn, USA) at a peak intensity of 350 and a duty factor of 2.0 for 1000 cycles (8 min). Cell debris and insoluble proteins were removed by centrifugation (13,000 rpm, 30 min at 5 °C). Furthermore, the PVM CP-derived proteins were separated from the cellular proteins by ultracentrifugation (SW28 rotor, Beckman, Palo Alto, USA; 25,000 rpm, 6 h, 5 °C) in a sucrose gradient (20–60 % sucrose in 20 mM Tris buffer, pH of 8.0) containing 1 % Triton X-100, 1 mM PMSF, and 5 mM β-mercaptoethanol. The gradient was divided into six fractions, which began at the bottom of the gradient, and the fractions were analyzed by SDS/PAGE. Fractions containing recombinant PVM coat protein (PvmCP) or its derivatives were combined and were dialyzed against 100 volumes of the same Tris buffer to remove the sucrose. After dialysis, PvmCP preparations were concentrated using an Amicon Ultra-15 centrifugal device (Ultracel 100 K; Millipore, Cork, Ireland). To obtain pure preparations of PvmCP or its derivatives for further study, the sucrose gradient, dialysis, and concentration steps were repeated. The concentrations of VLPs were estimated by densitometric comparison of recombinant PvmCP samples with a reference protein of known concentrations in Coomassie stained SDS/PAGE gels using the gel electrophoresis image analysis software (GelAnalyzer, 2010a freeware, www.gelanalyzer.com) or by UV spectroscopic measurements at 280 nm.

The obtained VLP solutions (3–5 mg/ml) were stored at −70 °C in a 20 mM Tris buffer (pH of 8.0). All steps involved in the expression and purification of the VLPs were monitored by SDS/PAGE using 12.5 % gels.

Electron Microscopy

For direct electron microscopy, purified PVM-derived proteins were adsorbed on carbon formvar-coated copper grids and were negatively stained with 1 % uranyl acetate aqueous solution. The grids were examined using a JEM-1230 electron microscope (JEOL, Tokyo, Japan) at an accelerating voltage of 100 kV.

For immunogold detection of Z-domain, purified PvmCP-NZ VLPs were incubated with Anti-rabbit IgG (whole molecule)-gold (5 nm) antibody produced in goat (Sigma, Saint Louis, USA) according to the procedure described in [26] and examined under electron microscope, as described above.

Mass Spectrometry Analysis

PVM CP-derived VLPs (1 mg/ml in 20 mM Tris buffer) were diluted with a 3-hydroxypicolinic acid matrix solution and were spotted onto an MTP AnchorChip 400/384TF. Matrix-assisted laser desorption/ionization (MALDI)-TOF mass spectrometry (MS) analysis was performed on an Autoflex MS (Bruker Daltonik, Bremen, Germany). The protein molecular mass calibration standard II (22.3–66.5 kDa; Bruker Daltonik) was used to determine the mass. The experimental data were compared with theoretical values of average protein molecular masses (MM) obtained using the PeptideMass tool (http://web.expasy.org/peptide_mass/).

VLP Characterization

The presence of nucleic acids in VLPs was evaluated in agarose gels: 20 µl of purified particle solution (1 mg/ml) was loaded in the pockets of 0.8 % agarose gel in the conventional Tris/sodium borate/EDTA (TBE) buffer. To prepare the disassembled VLPs, the particles were treated with 1 % SDS for 60 min at +37 °C. Nucleic acids in the gels were visualized with ethidium bromide (0.002 %, included in agarose gel) under UV light. To identify protein signals, the same agarose gels were stained with a solution containing 0.1 % Coomassie G-250, 10 % ethanol, and 10 % acetic acid and destained in the same solution without G-250.

For the analysis of the encapsidated nucleic acids, first unprotected RNAs and DNAs were removed from VLP preparations. 0.15 mg of PVM VLPs in 300 µl of a buffer that contained 50 mM Tris and 1 mM $MgCl_2$ with a pH of 7.0 was treated with 375U of Benzonase nuclease (Novagen, San Diego, USA) for 1 h at 37 °C. Next, the nucleic acids were isolated using TRI reagent and analyzed by RT-PCR as described previously using primer pairs 2F/2R (expected size of PCR fragment is 911 nt), 8F/8R (322 nt), and 9F/9R (484 nt).

The PVM VLP UV spectrum was recorded using a Nanodrop ND-1000 spectrophotometer (NanoDrop Technologies, Wilmington, USA).

For the VLP stability experiments, purified PvmCP VLPs (20 µl, 5 mg/ml) were added to 200 µl of the following solutions: Tris with a pH of 8.0, Tris + 1 M NaCl, Tris + 20 mM dithiothreitol, Tris + 20 mM EDTA, 100 mM Gly/HCl (pH of 2.5) or 100 mM CAPS (pH of 11) and incubated overnight at +4 °C. First, samples were centrifuged for 5 min at 13000 rpm; then, the 13 K-supernatants were transferred to ultracentrifuge tubes and spun at 72,000 rpm for 60 min at 5 °C in a TLA-100.1 rotor (Beckman, Palo Alto, USA). The 72 K-supernatants were removed, and the pellets were solubilized in the same volume of the Tris buffer. The presence of high molecular mass VLPs in the solutions after ultracentrifugation was assessed spectrophotometrically at 280 nm using a Nanodrop ND-1000 device.

To test the VLP stability under different chemical conditions and temperatures, the structural changes in PVM CP-derived VLPs were monitored in buffer solutions containing 20 mM Tris (pH of 8.0), Tris + 1 M NaCl, Tris + 20 mM EDTA; Tris + 20 mM dithiothreitol (DTT) in the presence of Sypro Orange dye (1:400 dilution of stock solution, Sigma, Saint Louis, USA) using a DNA melting point determination program and a real-time PCR system MJ Mini (Bio-Rad, Hercules, USA), as described previously [12].

IgG Binding Studies

Naïve rabbit serum was used as the IgG source, which was obtained in compliance with the Latvian Animal Protection Law and a certificate from the Food and Veterinary Service that was issued based on a decision by the Council for Ethical Treatment of Animals in Latvia.

To test the IgG binding activity of PvmCP-NZ VLPs, 100 µl of rabbit serum was added to 900 µl of the solution containing 3 mg/ml PvmCP-NZ in 20 mM Tris buffer (pH of 8.0) supplemented with 1 mM PMSF. The resulting solution was incubated for 18 h at +4 °C. The control samples contained the same components without VLPs or PvmCP VLPs without the Z-domain. After incubation, all samples were separated at 25,000 rpm for 6 h at 5 °C (SW40 rotor, Beckman, Palo Alto, USA) in a sucrose gradient (20–60 % sucrose in 20 mM Tris buffer, pH of 8.0) that contained 1 mM PMSF. After fractionation, the gradient samples were analyzed in SDS/PAGE gel and after the transfer onto a Hybond-C nitrocellulose membrane (GE Healthcare, Piscataway, USA) by a Western blot. To identify IgG signals on the blot, the membranes were incubated at room temperature for 3 h with horseradish peroxidase-conjugated anti-rabbit IgG against an entire antibody molecule developed in a goat (Sigma, Saint Louis, USA) that was diluted 1:1000 in PBS. The signal bands were visualized by incubating the membrane in the TBS buffer supplemented with peroxidase substrates (0.002 % *o*-dianisidine and 0.03 % hydrogen peroxide).

Results and Discussion

cDNA Cloning, Expression of PVM CP Derivatives, VLP Identification, and Initial Characterization

The carlavirus PVM coat protein is synthesized from ORF5 of the virus genome. The primers for the RT-PCR cloning

of the CP gene were chosen on the basis of PVM sequence alignments upstream of the start codon and downstream of the CP gene as described in the "Materials and methods" section. After cloning and sequencing analysis, we found that our PVM CP variant differed from all published PVM sequences; the closest isolates are the Tanzania isolate (TZ:PVM12U:11; Genbank KC866622, identity 97 % on cDNA level) and Iran isolate PVM-352 (Genbank JX678982; identity 99 % on AA sequence level). According to the classification, our isolate belongs to the PVM-o evolutionary lineage [18].

All PVM CP-derived expression vectors were constructed as described in the "Materials and methods" section. Taking into account our previous experience in creating nanomaterials from filamentous viruses [12], we decided to add a long flexible AA linker $(G4S)_3$ to the N- or C-terminus of the PVM CP. Additionally, to evaluate the suitability of a VLP carrier to display foreign AA, it is necessary to demonstrate the capacity of the carrier to accommodate sequences of a defined length without influencing VLP formation. As a model protein for the capacity test, we chose ZZ-domain (116 AA) of the IgG binding protein A from *S. aureus*. This protein is stable and can be obtained in soluble form from recombinant *E. coli* cells after expressing the ZZ gene [27]. In our experiments, the ZZ gene was genetically fused to the 5′-end of CP gene with a $(G4S)_3$ encoding spacer (deduced AA sequences can be found in Fig. 1 of the Suppl.).

After introducing the vectors in the *E.coli* expression strain, the cells were cultivated at +20 °C, and the obtained biomass was treated with ultrasound to obtain cell lysates. As revealed by the SDS/PAGE analysis and following densitometric evaluations, the chosen cultivation conditions ensured the localization of approximately 40 % of the target protein in the soluble fraction of the cell lysate (a typical example is shown in Suppl. Figure 2). Subsequent sucrose gradient analysis revealed that a significant part (approximately 25 %) of the target protein was found in the bottom fractions of the gradient (40–60 % sucrose), which suggests the presence of soluble PvmCP aggregates with high molecular masses.

After repeated gradient purification and ultrafiltration steps, the output of the purified PvmCP and its derivatives varied between 20 and 30 mg/l or 1.6–2.5 mg/g wet biomass. These data suggest that the yield of PVM VLPs from bacterial expression system is more than 30 times better compared to virus outputs from PVM-infected plants [21].

The PvmCP and its derivative preparations after SDS/PAGE (Fig. 1a) were further analyzed by UV spectrometry, agarose gel, RT-PCR, and mass spectrometry.

UV spectrometric analysis of purified PvmCP (Fig. 1b) demonstrated a weak maximum at 260 nm (OD260/OD280 = 1.12), which indicates the presence of protein/nucleic acid complexes in the preparation. Additional agarose gel analysis (Fig. 1c) revealed extremely weak or no nucleic acid signal after staining with ethidium bromide in the case of both tested proteins (PvmCP and PvmCP-NZ, Fig. 1c, lanes 1 and 3), which could be clearly observed after denaturation with 1 % SDS (lanes 2 and 4). Subsequent Coomassie staining of the gel demonstrated overlapping signals, which suggests the co-localization of protein and nucleic acid components, which is characteristic for viruses and VLPs. It is known that the native PVM RNA content is comparably low (5–6 % of particle weight, [21]), whereas for such an icosahedral plant virus as CCMV, the RNA content reaches 24 % of the particle weight [28]. Our PVM CP preparations contain approximately 3 % nucleic acids, taking into account the output of nucleic acids (33 μg from 1 mg of PvmCP) after Benzonase and TRI reagent treatment (see "Materials and Methods" section).

Considering the data regarding the low RNA content in PVM CP preparations, the weak signals in agarose gel can be explained by the low amounts of nucleic acids in the preparations and by the possible tight packaging of nucleic acids inside of the PVM CP complexes that prevent efficient ethidium bromide staining.

To identify the RNA species in PvmCP/nucleic acid complexes, the presence of three major RNAs from the constructed *E.coli* expression system was tested in a purified PvmCP sample (Fig. 1d). To remove the unprotected nucleic acids from the preparation, the Benzonase nuclease was used before the RNA isolation from the PvmCP as described in the "Materials and Methods" section. After RNA purification and RT-PCR, specific PCR products of the expected size were obtained in all tested cases, which indicate the presence of PvmCP mRNA, 16S rRNA, and 23S rRNA in the samples. However, because PvmCP was purified using sucrose gradient centrifugation, we cannot exclude the presence of low amounts of contaminating ribosomes because ribosomes can also be efficiently co-purified by sucrose gradient centrifugation [29]. Therefore, the existence of PvmCP-protected rRNA is questionable. More exact identification of nucleic acid species can be performed using an alternative purification scheme for PVM VLPs and next-generation sequencing technique, which has been shown for the case of a single-stranded RNA virus (flock house virus) [30].

Furthermore, purified PvmCP and its derivatives were subjected to mass spectrometric analysis (MS). Data obtained in the analysis of unmodified PvmCP (Fig. 1e, panel 1) demonstrate that the experimentally determined protein molecular mass (MM; 33708.2) approximately corresponds to the calculated MM value for the protein without N-terminal Met (33719.9), which is typical for *E.coli*-produced recombinant proteins if the second AA is

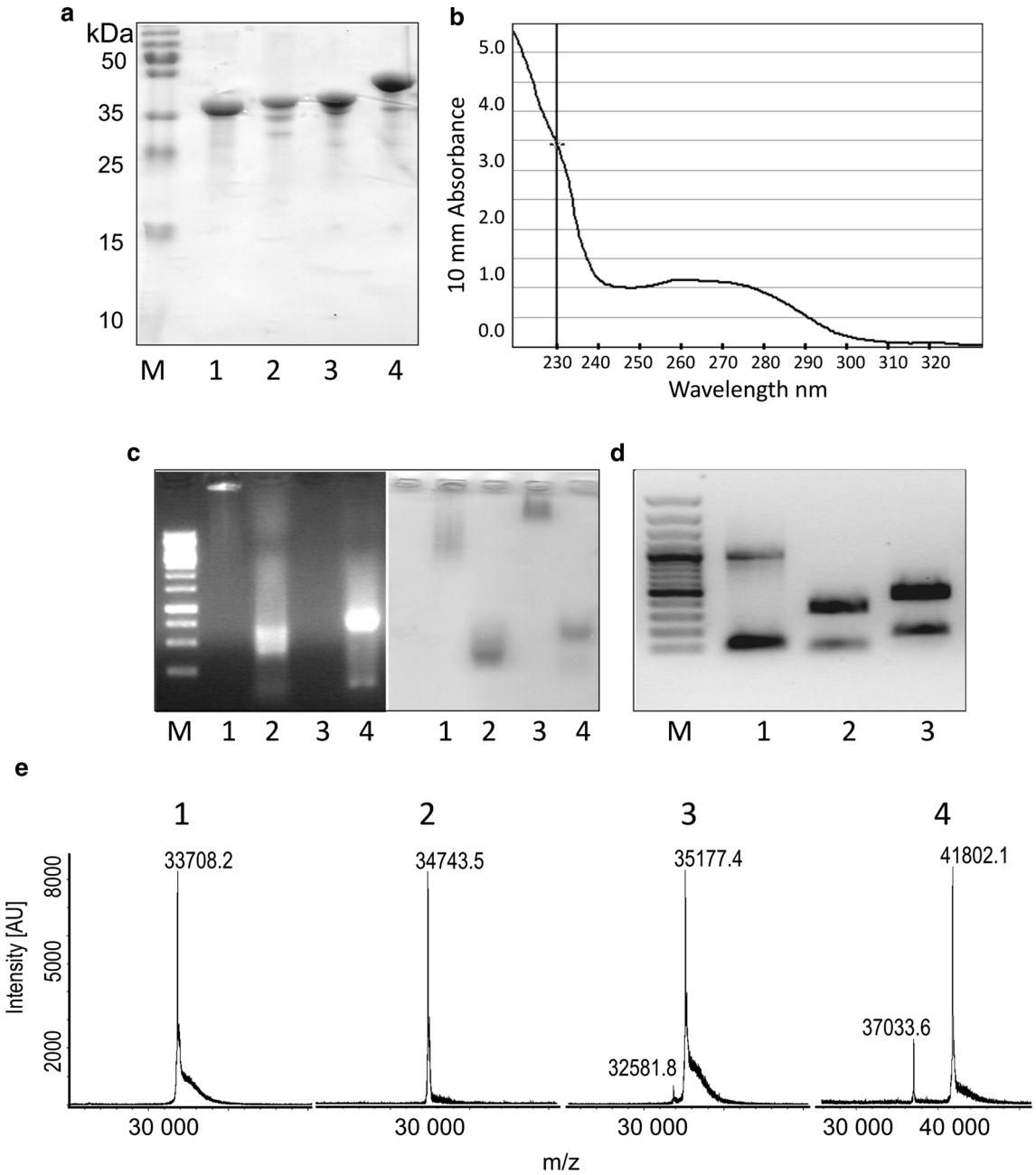

Fig. 1 Properties of PVM-derived proteins. **a** SDS/PAGE analysis of PVM CP-derived proteins following expression of the appropriate genes in *E.coli* C2566 cells and purification: PvmCP (*lane 1*); PvmCP-CG4S (*lane 2*), PvmCP-NG4S (*lane 3*), PvmCP-NZ (*lane 4*), protein MM marker (*lane M*) (Fermentas, Vilnius, Lithuania); **b** UV spectrum of purified PvmCP. **c** Agarose gel analysis of native PvmCP after purification (*lane 1*), SDS-denatured PvmCP (*lane 2*), native PvmCP-NZ after purification (*lane 3*), SDS-denatured PvmCP-NZ (*lane 4*), 1 kb DNA size marker (Fermentas, Vilnius, Lithuania, lane M); *left* ethidium bromide stained gel, *right* Coomassie stained gel. **d** RT-PCR analysis of nucleic acids in purified and Benzonase nuclease-treated PvmCP preparations. Nucleic acids after isolation using TRI reagent were amplified with PVM CP-specific primers (2F/2R, *lane 1*), *E.coli* 16S ribosomal primers (8F/8R, *lane 2*), and 23S ribosomal primers (9F/9R, *lane 3*), as described in the "Materials and methods" section. In *lane M*, 100 bp DNA size marker (Fermentas, Vilnius, Lithuania) was loaded. **e** Mass spectrometry analysis of purified PVM CP-derived proteins: PvmCP (*panel 1*), PvmCP-CG4S (*panel 2*), PvmCP-NG4S (*panel 3*), PvmCP-NZ (*panel 4*)

glycine [31]. In the case of PvmCP-CG4S, a larger difference between the calculated value and experimental MS data was observed (34809.4/34743.5, Fig. 1e, panel 2). The addition of the N-terminal G4S sequence to the PvmCP also resulted in a smaller sized protein (35226.49/35177.5; Fig. 1e, panel 3). MS analysis of the PvmCP-NZ

demonstrated a difference of approximately 6.7 kDa between the calculated and experimental MM value (48463.2/41802.1; Fig. 1e, panel 4), which suggests significant proteolytic degradation of the target protein during cultivation and purification. Assuming that the C-terminal part of the protein is unchanged, the obtained PvmCP-NZ preparation should still contain one complete Z-domain instead of the expected double-Z-domain and a minor product (37033.6) that contains residual C-terminal 20 AA stretch from the Z-domain (Suppl. Figure 1d).

The differences between the calculated and obtained MM can be explained by AA sequence analysis. The PvmCP contains 3 Cys and 9 Met residues (Suppl. Figure 1a); if they are chemically oxidized after the purification process [32], the interpretation of the MS data becomes more complicated. Therefore, additional mass spectrometric analysis of tryptic peptides is necessary to obtain more exact AA sequence data of PvmCP-derived proteins, as shown, for example, with plant virus BMV [33].

Furthermore, the purified PvmCP and its derivatives were examined under an electron microscope. As shown in Fig. 2, in all cases, filamentous VLPs were found, which morphologically resemble native PVM virions. The measured approximate particle diameter was 13 nm for the PvmCP VLPs, and the filament lengths were between 30 and 800 nm; however, more than 60 % of the VLPs were in the 100–300 nm range (Suppl. Figure 3). Similarly to PVY-like particles [12], additionally, PvmCP is able to form even longer VLPs than native virions (up to 820 nm).

Comparable VLP dimensions were also observed for PvmCP-NG4S and PvmCP-NZ. For VLPs with a C-terminal G4S-linker, the morphology of particles was found to have strongly changed into short fragments (Fig. 2c), which suggests that the addition of even a short AA linker sequence to the C-terminal end of the PvmCP leads to a significant reduction in VLP lengths. Therefore, the C-terminal variant was not further considered as a carrier of foreign sequences due to the low output of typical VLP structures.

Additionally, we tested the surface location of introduced Z-domain and IgG binding using gold-labeled antibodies as described in "Materials and Methods" section. As seen in EM images (Fig. 2f, g), all the PvmCP-NZ VLPs were decorated with 5-nm-gold-conjugated IgGs, whereas only few gold particles were identified on EM image in control experiment with PvmCP VLPs.

Stability of PVM VLPs

The purification procedures used in this study clearly demonstrate the stability of PVM VLPs under physiological conditions and at −70 °C. To obtain more information regarding the stability of particles at different conditions, we used two independent methods: (i) incubations of PvmCP VLPs in different buffer solutions with subsequent ultracentrifugation and (ii) temperature-dependent binding of Sypro Orange dye to the hydrophobic AA regions of PvmCP-derived proteins using a real-time thermal cycler as an instrument for fluorescence recording at elevated temperatures.

The results of the incubation experiments (Fig. 3) demonstrated that such buffer conditions as high salt and basic (pH of 11) solutions as well as reducing (DTT) and chelating agents (EDTA) did not cause the disassembly of VLPs in non-sedimenting CP monomers and/or oligomers. The only exception was the low-pH Gly-buffer, which indicates that these conditions may support the disassembly of PvmCP VLPs. Additionally, for certain other VLPs, strongly acidic conditions are necessary to achieve particle disassembly in CP oligomers, as shown with bacteriophage MS2 [34]. These experiments show that low-pH conditions can be used for purification of PvmCP monomers/oligomers for subsequent reassembly experiments with chosen active agents, e.g., nucleic acids, negatively charged polymers, and other substances for packaging inside PVM-like nanoparticles.

The principle of stability tests using Sypro Orange can be explained as follows: a solution containing VLPs does not activate Sypro Orange fluorescence at room temperature (hydrophobic AA stretches of CP are hidden). Thermal denaturation exposes the hydrophobic surfaces of the VLPs and stimulates Sypro Orange binding and fluorescence. Therefore, the VLP stability curve can be obtained by changing the temperature gradually to unfold the protein and measure the change in fluorescence. The results are expressed as negative increments of fluorescence with time (Suppl. Figure 4). PvmCP VLP incubations with Sypro Orange at different conditions and increasing temperatures indicated several important properties of newly constructed VLPs. The most significant changes were observed (as minima in the corresponding spectrum) at 52–54 °C for PvmCP or its N-terminal derivatives, whereas the C-terminal CG4S derivate bound the majority of the fluorescent dye at 41 °C. These results are in good agreement with EM studies, where mostly unstable, short VLP filaments were found. In all cases, increased salt concentration stabilized the particles, whereas EDTA did not influence the temperature stability. This observation suggests that possibly, bivalent cations are unnecessary for particle stabilization. Several minima found in the case of the DTT-containing buffer likely reflect a gradual reduction of putative disulfide bounds in the VLP structure.

The thermal inactivation point of native PVM was estimated to be within the range 60–71 °C, as shown in experiments with thermally treated virus samples and

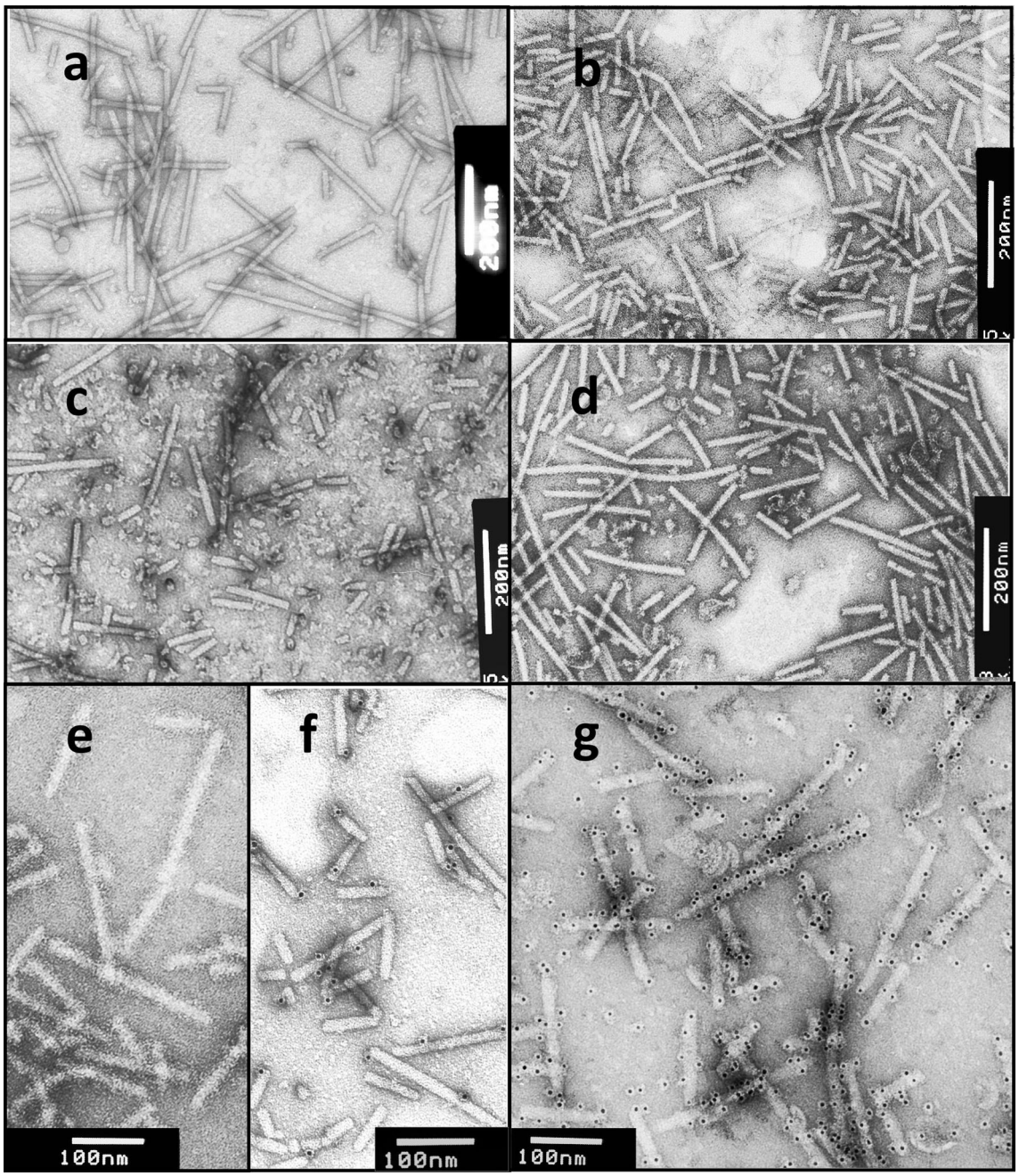

Fig. 2 Electron micrographs of PVM CP-derived VLPs. **a** Purified VLPs formed from PVM CP after expression of the PvmCP gene; **b** PvmCP VLPs with N-terminal G4S-linker (PvmCP-NG4S); **c** PvmCP VLPs with C-terminal G4S-linker (PvmCP-CG4S); **d** PvmCP displaying *Staphylococcus aureus* Z-domain (PvmCP-NZ); **e** PvmCP-NZ after incubation with naïve rabbit serum; **f** PvmCP VLPs after incubation with Anti-rabbit IgG (whole molecule)-gold antibody (control experiment); **g** PvmCP-NZ VLPs after incubation with Anti-rabbit IgG (whole molecule)-gold antibody. *Bar* 200 nm (**a**, **b**, **c**, **d**), 100 nm (**e**, **f**, **g**)

inoculated test plants [35]. Assuming that the reduction in infectivity is bound with temperature-depending changes in virion structure, the observed "melting point" of PVM VLPs at 52–54 °C obtained in the Sypro Orange experiments can be compared with the thermal inactivation point of native PVM. Therefore, artificially constructed PVM VLPs are apparently less stable than their native progenitor virus.

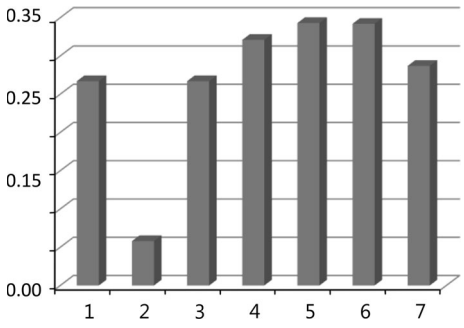

Fig. 3 Stability studies of PvmCP-derived VLPs. VLPs were incubated in the following buffer solutions: 20 mM Tris (pH of 8.0, *bar 1*), 100 mM Gly/HCl (pH of 2.5, *bar 2*), 100 mM CAPS (pH of 11, *bar 3*), Tris buffer + 1 M NaCl (*bar 4*), Tris buffer + 20 mM EDTA (*bar 5*), Tris buffer + 20 mM dithiothreitol (*bar 6*) and Tris buffer + 20 mM EDTA + 20 mM dithiothreitol (*bar 7*). Then, VLPs were sedimented by ultracentrifugation and solubilized, and the relative concentrations of pelleted VLPs were estimated spectrophotometrically at 280 nm, as described in the "Materials and methods" section

IgG Binding to the Z-Domain Containing PVM VLPs

The Z-domain is an artificial protein derived from domain B found in *S. aureus* A protein, which is able to specifically interact with immunoglobulins in a non-antigenic manner. To confirm the ability of Z-domain containing PVM VLPs to bind native IgGs, we chose the naïve rabbit serum as the IgG source due to strong interaction between *S. aureus* protein A to the Fc region of rabbit IgGs [36].

The binding tests were performed as described in the "Materials and methods" section, and the results of the analysis are shown in Fig. 4. At sucrose gradient conditions, without VLPs, the signals of IgG heavy chains (approximately 50 kDa, arrows in Fig. 4) were found in upper part of the gradient (0–20 % sucrose). The same IgG localization was found when IgGs were incubated with unmodified PvmCP VLPs, which suggests that rabbit IgGs do not recognize PvmCP VLPs. When PvmCP-NZ VLPs were used as the binding partner, IgG-specific zones disappeared from the top of gradient and were found co-localized with the VLP fractions (40–50 % sucrose), which indicates the specific interaction between both proteins. Subsequent densitometric analysis of signals in Coomassie stained gels revealed that the signal intensity of IgG heavy chains was approximately 20 % of that of CP. Taking in account the molecular masses of IgGs (approx.150 kDa) and PvmCP-NZ (42 kDa), the calculation results in the assumption that one IgG molecule is bound to every fifth CP-subunit of the VLPs. To achieve more efficient binding, additional optimization experiments are necessary, as suggested in [37].

Interestingly, when denatured at Western blot conditions, the Z-domain that was fused to PvmCP was still able to bind to peroxidase-conjugated goat secondary antibodies, which also allowed visualization of the PvmCP-NZ zones in the blot. Parallel to these experiments, PvmCP-NZ VLPs after incubation with rabbit serum and purification in the sucrose gradient were tested in the EM. As seen from

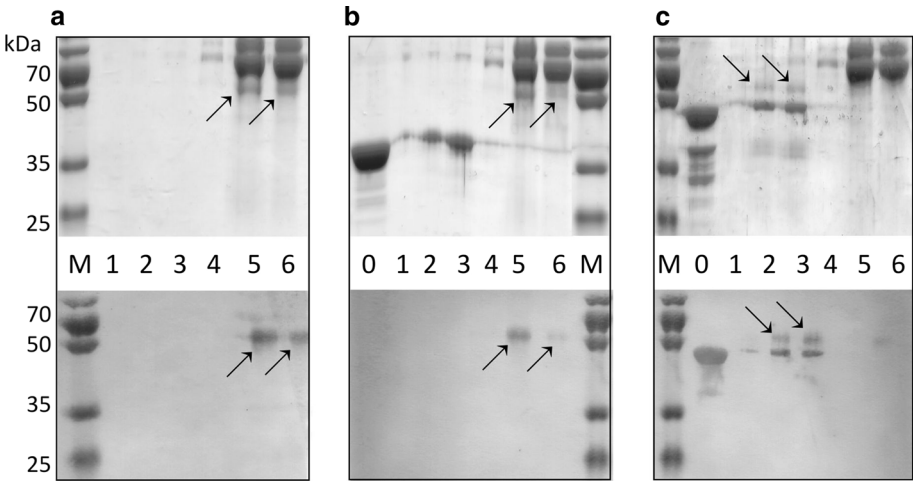

Fig. 4 SDS/PAGE and Western blot analysis of IgG binding to PvmCP-NZ VLP carrier. Rabbit serum was incubated with PvmCP-NZ VLPs (**c**), as described in the "Materials and methods" section. Control samples contained the same components without VLPs (**a**) or PvmCP VLPs without a Z-domain (**b**). After incubation, all samples were separated in a sucrose gradient using an ultracentrifuge SW40 rotor. The gradient fractions were analyzed in SDS/PAGE gel (*top of the panel*) and a Western blot analysis (*bottom of the panel*). To identify the IgG signals on the blot, the horseradish peroxidase-conjugated anti-rabbit IgG against whole antibody and *o*-dianisidine was used. The *arrows* denote the relative localization of the IgG heavy chain on the blots. *Lane M* protein MM marker; *lane 0* PvmCP (**b**) or PvmCP-NZ VLPs (**c**) before the incubation with IgG; *lanes 1–6* sucrose gradient fraction from the bottom of the tube (1–60, 2–50, 3–40, 4–30, 5–20, 6–0 % sucrose)

the EM image (Fig. 2e), VLPs without signs of aggregation, filament fragmentation, or disassembly were found after being incubated with rabbit serum. From the initially intended ZZ-domain (139 AA), after proteolytic processing, it was found that only 78 AAs were fused to PVM CP, which represents at least one functionally active Z-domain. This domain apparently is located on the surface of filaments and efficiently binds with rabbit IgGs. Additional immunogold electron microscopy experiments confirmed that Z-domain is accessible to IgG molecules (Fig. 2g). The IgG binding ability of viral nanoparticles with introduced functional parts of protein A has already been demonstrated previously in work with modified plant tobamovirus TVCV [37] and bacteriophage Qβ VLPs [38].

Concluding Remarks

In this study, we demonstrated the construction, purification, and initial characterization of a new filamentous VLP carrier through the cloning and expression of the plant virus PVM structural gene in *E. coli*. To the best of our knowledge, it is the first report about *Carlavirus* genus-derived VLPs from a bacterial expression system. Moreover, the chosen expression system allowed VLPs to be obtained in yields, more than 30 times exceeding the output of the virus from native plant system.

Experiments on the structural and functional characterization of the obtained particles revealed the important property of the PVM VLP carrier: the ability to accommodate comparably long, functionally active protein domains at the N-terminal part of the CP on the VLP surface without influencing the VLP morphology. Therefore, different peptide and protein ligands can be introduced in the VLP structure, where the goal is to construct new vaccine carrier candidates and nanomaterials. Despite the necessary immunological characterization of the PVM VLP carrier being still incomplete, the first mice immunization experiments suggest a significant immune response against unmodified PVM VLPs without adjuvant usage (data not shown), which is even stronger than that of previously reported PVY VLPs [12]. Additionally, taking into account the presence of Lys-residues at possibly surface-exposed N-terminus of PVM CP, one could expect that the necessary functional molecules can be introduced in the PVM VLP structure also by means of chemical coupling.

Next, using a RT-PCR test, we found that among nucleic acids packaged inside of the particles, PVM VLPs contain the mRNA of CP. The stability tests of PVM VLP derivatives suggest further advantages of the carrier, such as the ability to withstand high ionic strength and a high pH environment as well as chelating and reducing agents in solutions. Moreover, low-pH buffer systems can be a starting point for optimization experiments, where the goal is for disassembly and packaging different active compounds inside of PVM VLPs. Finally, we demonstrated that the constructed Z-domain containing PVM VLPs after corresponding optimizations can be used for the immobilization of different antibodies as universal carriers to create new diagnostic tools in the future.

Acknowledgments The authors wish to thank Prof. Dr. P. Pumpens for critical reading of the manuscript and suggestions, Prof. Dr. K. Tars and Dr. A. Kazaks for helpful discussions. G. Grinberga, G. Resevica, and V. Zeltina are acknowledged for their technical assistance. This work was supported by the ERAF Grant 2013/0052/2DP/2.1.1.1.0/13/APIA/VIAA/019.

References

1. Zeltins, A. (2013). Construction and characterization of virus-like particles: a review. *Molecular Biotechnology, 53*, 92–107.
2. Pushko, P., Pumpens, P., & Grens, E. (2013). Development of virus-like particle technology from small highly symmetric to large complex virus-like particle structures. *Intervirology, 56*, 141–165.
3. Zhao, Q., Li, S., Yu, H., Xia, N., & Modis, Y. (2013). Virus-like particle-based human vaccines: Quality assessment based on structural and functional properties. *Trends in Biotechnology, 31*, 654–663.
4. Jain, N. K., Sahni, N., Kumru, O. S., Joshi, S. B., Volkin, D. B., & Middaugh, C. R. (2014). Formulation and stabilization of recombinant protein based virus-like particle vaccines. *Advanced Drug Delivery Reviews,*. doi:10.1016/j.addr.2014.10.023.
5. Liu, F., Ge, S., Li, L., Wu, X., Liu, Z., & Wang, Z. (2012). Virus-like particles: Potential veterinary vaccine immunogens. *Research in Veterinary Science, 93*, 553–559.
6. Haynes, J. R., Cunningham, J., von Seefried, A., Lennick, M., Garvin, R. T., & Shen, S. H. (1986). Development of a genetically-engineered, candidate polio vaccine employing the self assembling properties of the tobacco mosaic virus coat protein. *Biotechnology, 4*, 637–641.
7. Lomonossoff, G. P., & Evans, D. J. (2014). Applications of plant viruses in bionanotechnology. *Current Topics in Microbiology and Immunology, 375*, 61–87.
8. Namba, K., & Stubbs, G. (1986). Structure of tobacco mosaic virus at 3.6 A resolution: Implications for assembly. *Science, 231*, 1401–1406.
9. Kendall, A., McDonald, M., Bian, W., Bowles, T., Baumgarten, S. C., Shi, J., et al. (2008). Structure of flexible filamentous plant viruses. *Journal of Virology, 82*, 9546–9554.
10. Cruz, S. S., Chapman, S., Roberts, A. G., Roberts, I. M., Prior, D. A., & Oparka, K. J. (1996). Assembly and movement of a plant virus carrying a green fluorescent protein overcoat. *Proceedings of the National Academy of Sciences, 93*, 6286–6290.
11. Denis, J., Majeau, N., Acosta-Ramirez, E., Savard, C., Bedard, M. C., Simard, S., et al. (2007). Immunogenicity of papaya mosaic virus-like particles fused to a hepatitis C virus epitope: Evidence for the critical function of multimerization. *Virology, 363*, 59–68.
12. Kalnciema, I., Skrastina, D., Ose, V., Pumpens, P., & Zeltins, A. (2012). Potato virus Y-like particles as a new carrier for the

presentation of foreign protein stretches. *Molecular Biotechnology, 52*, 129–139.
13. Saini, M., & Vrati, S. (2003). A Japanese encephalitis virus peptide present on Johnson grass mosaic virus-like particles induces virus-neutralizing antibodies and protects mice against lethal challenge. *Journal of Virology, 77*, 3487–3494.
14. Turpen, T. H., Reinl, S. J., Charoenvit, Y., Hoffman, S. L., Fallarme, V., & Grill, L. K. (1995). Malaria epitopes expressed on the surface of recombinant tobacco mosaic virus. *Nature Biotechnology, 13*, 53–57.
15. Brown, A. D., Naves, L., Wang, X., Ghodssi, R., & Culver, J. N. (2013). Carboxylate-directed in vivo assembly of virus-like nanorods and tubes for the display of functional peptides and residues. *Biomacromolecules, 14*, 3123–3129.
16. Lee, K. L., Shukla, S., Wu, M., Ayat, N. R., El Sanadi, C. E., Wen, A. M., & Steinmetz, N. F. (2015). Stealth filaments: Polymer chain length and conformation affect the in vivo fate of PEGylated potato virus X. *Acta Biomaterialia, 19*, 166–179.
17. Zavriev, S. K., Kanyuka, K. V., & Levay, K. E. (1991). The genome organization of potato virus M RNA. *Journal of General Virology, 72*, 9–14.
18. Tabasinejad, F., Jafarpour, B., Zakiaghl, M., Siampour, M., Rouhani, H., & Mehrvar, M. (2014). Genetic structure and molecular variability of potato virus M populations. *Archives of Virology, 159*, 2081–2090.
19. Brandes, J., Wetter, C., Bagnall, R. H., & Larson, R. H. (1959). Size and shape of the particles of Potato virus S, Potato virus M, and Carnation latent virus. *Phytopathology, 49*, 443–446.
20. Veerisetty, V., & Brakke, M. K. (1977). Differentiation of legume carlaviruses based on their biochemical properties. *Virology, 83*, 226–231.
21. Tavantzis, S. M. (1983). Improved purification of two potato carlaviruses. *Phytopathology, 73*, 190–194.
22. Naylor, M., Reeves, J., Cooper, J. I., Edwards, M. L., & Wang, H. (2005). Construction and properties of a gene-silencing vector based on Poplar mosaic virus (genus Carlavirus). *Journal of Virological Methods, 124*, 27–36.
23. Eastwell, K. C., & Druffel, K. L. (2012). Complete genome organization of American hop latent virus and its relationship to carlaviruses. *Archives of Virology, 157*, 1403–1406.
24. Wang, R., Wang, G., Zhao, Q., Zhang, Y., An, L., & Wang, Y. (2010). Expression, purification and characterization of the Lily symptomless virus coat protein from Lanzhou Isolate. *Virology Journal, 7*, 34.
25. Sambrook, J., & Russell, D. W. (2001). *Molecular cloning: A laboratory manual* (3rd ed.). New York: Cold Spring Harbor.
26. Louro, D., & Lesemann, D. E. (1984). Use of protein A-gold complex for specific labelling of antibodies bound to plant viruses. I. Viral antigens in suspensions. *Journal of Virological Methods, 9*, 107–122.
27. Nilsson, B., Moks, T., Jansson, B., Abrahmsen, L., Elmblad, A., Holmgren, E., et al. (1987). A synthetic IgG-binding domain based on staphylococcal protein A. *Protein Engineering, 1*, 107–113.
28. Bancroft, J. B., Hiebert, E., Rees, M. W., & Markham, R. (1968). Properties of cowpea chlorotic mottle virus, its protein and nucleic acid. *Virology, 34*, 224–239.
29. Ederth, J., Mandava, C. S., Dasgupta, S., & Sanyal, S. (2009). A single-step method for purification of active His-tagged ribosomes from a genetically engineered *Escherichia coli*. *Nucleic Acids Research, 37*, e15.
30. Routh, A., Domitrovic, T., & Johnson, J. E. (2012). Host RNAs, including transposons, are encapsidated by a eukaryotic single-stranded RNA virus. *Proceedings of the National Academy of Science of the United States of America, 109*, 1907–1912.
31. Hirel, P. H., Schmitter, M. J., Dessen, P., Fayat, G., & Blanquet, S. (1989). Extent of N-terminal methionine excision from *Escherichia coli* proteins is governed by the side-chain length of the penultimate amino acid. *Proceedings of the National Academy of Science of the United States of America, 86*, 8247–8251.
32. Kotiaho, T., Eberlin, M. N., Vainiotalo, P., & Kostiainen, R. (2000). Electrospray mass and tandem mass spectrometry identification of ozone oxidation products of amino acids and small peptides. *Journal of the American Society for Mass Spectrometry, 11*, 526–535.
33. Ni, P., Vaughan, R. C., Tragesser, B., Hoover, H., & Kao, C. C. (2014). The plant host can affect the encapsidation of brome mosaic virus (BMV) RNA: BMV virions are surprisingly heterogeneous. *Journal of Molecular Biology, 426*, 1061–1076.
34. Glasgow, J. E., Capehart, S. L., Francis, M. B., & Tullman-Ercek, D. (2012). Osmolyte-mediated encapsulation of proteins inside MS2 viral capsids. *ACS Nano, 6*, 8658–8664.
35. Ahmad, I., Stace-Smith, R., & Wright, N. S. (1985). Some properties of potato virus M (PVM) in crude sap and in pure preparations. *Pertanika, 8*, 73–77.
36. Brown, N. L., Bottomley, S. P., Scawen, M. D., & Gore, M. G. (1998). A study of the interactions between an IgG-binding domain based on the B domain of staphylococcal protein A and rabbit IgG. *Molecular Biotechnology, 10*, 9–16.
37. Werner, S., Marillonnet, S., Hause, G., Klimyuk, V., & Gleba, Y. (2006). Immunoabsorbent nanoparticles based on a tobamovirus displaying protein A. *Proceedings of the National Academy of Science of the United States of America, 103*, 17678–17683.
38. Brown, S. D., Fiedler, J. D., & Finn, M. G. (2009). Assembly of hybrid bacteriophage Qβ virus-like particles. *Biochemistry, 48*, 11155–11157.